

***p*-wave stabilization of three-dimensional Bose-Fermi solitons**

N. G. Parker*

School of Mathematics and Statistics, Newcastle University, Newcastle Upon Tyne NE1 7RU, United Kingdom

D. A. Smith

Vienna Center for Quantum Science and Technology, Atominstiut, TU Wien, A-1020 Vienna, Austria

(Received 17 August 2011; published 3 January 2012)

We explore bright soliton solutions of ultracold Bose-Fermi gases, showing that the presence of *p*-wave interactions can remove the usual collapse instability and support stable soliton solutions that are global energy minima. A variational model that incorporates the relevant *s*- and *p*-wave interactions in the system is established analytically and solved to probe the dependencies of the soliton stationary states on key experimental parameters. Under attractive *s*-wave interactions, bright solitons exist only as metastable states susceptible to collapse. Remarkably, the presence of repulsive *p*-wave interactions alleviates this collapse instability. This dramatically widens the range of experimentally achievable soliton solutions and indicates greatly enhanced robustness. While we focus specifically on the boson-fermion pairing of ^{87}Rb and ^{40}K , the stabilization inferred by repulsive *p*-wave interactions should apply to the wider remit of ultracold Bose-Fermi mixtures.

DOI: [10.1103/PhysRevA.85.013604](https://doi.org/10.1103/PhysRevA.85.013604)

PACS number(s): 03.75.Lm, 67.85.Pq

I. INTRODUCTION

The study of wave mechanics and propagation in nonlinear media is a fundamental concept within physics. In particular, solitons are a general nondispersive solution to the one-dimensional nonlinear wave equation. Bright solitons have been observed in many areas of physics, such as in water [1], liquid hydrogen [2], optics [3], and atomic Bose-Einstein condensates (BECs) [4–6]. In the latter case, these self-trapped matter waves are supported by a balance between attractive atomic scattering interactions and repulsive zero-point kinetic energy between bosons. As well as being of fundamental interest in many-body quantum physics, bright matter-wave solitons are being touted for potential uses in atom interferometry [4,5,7,8] and surface characterization [9]. However, when realized in three-dimensions these solitons exist only as metastable states prone to catastrophic collapse [10,11].

Ultracold Bose-Fermi (BF) gases have received a great deal of recent experimental attention and have been realized through ^7Li - ^6Li [12], ^{23}Na - ^6Li [13], ^{87}Rb - ^{40}K [14], ^{174}Yb - ^{173}Yb [15], and ^{84}Sr - ^{87}Sr [16] mixtures. At such low temperatures, the scattering of atoms with nonzero relative angular momentum is heavily restricted such that *p*-wave and higher interactions are typically negligible. Furthermore, the Pauli exclusion principle forbids identical fermions from interacting via *s*-wave collisions. Thus, for an ultracold Bose-Fermi mixture (in which the fermions are identical), the dominant interactions are *s*-wave boson-boson and boson-fermion interactions. It has been shown theoretically that a repulsive Bose gas and a noninteracting Fermi gas coexisting in a radial waveguide can be coupled together by an attractive boson-fermion interaction to form a self-bound state in which the components are co-localized in space [17–19]. It is these “Bose-Fermi solitons” that we will consider in this paper. Note that distinct types of solitons have been predicted in Bose-Fermi mixtures, i.e., those supported in the presence

of an optical lattice [20] and those corresponding to a localized Bose gas embedded within an extended fermionic background [21].

However, just as in the case of an attractively interacting 3D Bose-Einstein condensate [10,11,22], a 3D Bose-Fermi system is prone to collapse when the interspecies interaction becomes too attractive [23–26]. While certain effects have been highlighted to raise the threshold for collapse, e.g., finite temperature effects in Bose-Fermi mixtures [27] and Feshbach resonance management [28], possession of angular momentum [29], and fragmentation [30] in Bose-Einstein condensates, the instability to collapse ultimately remains in the system. Indeed, by considering these 3D effects, Karpiuk *et al.* [18] confirmed that Bose-Fermi solitons are unstable to collapse when the attractive Bose-Fermi interactions become too strong. This showed that the soliton solutions exist only within a narrow range of interaction strengths and atom numbers, but these predictions included only *s*-wave interactions.

The ^{87}Rb - ^{40}K system appears particularly well suited to support BF solitons since its natural boson-fermion interaction is strongly attractive. Furthermore, by exploiting scattering resonances, the *p*-wave interaction between fermions can now be experimentally engineered to significant values [31]. It is, thus, the rationale of this work to explore the way in which *p*-wave interactions may modify Bose-Fermi soliton solutions. In order to obtain the stationary soliton solutions we perform a variational approach using a cylindrically symmetric Gaussian ansatz for the boson and fermion density distributions. Via the Gross-Pitaveskii model for the bosons and the Thomas-Fermi approximation for the fermions, we derive an analytic form for the energy of this coupled system up to *p*-wave interactions (for the boson-fermion and fermion-fermion interaction).

Written in terms of a generalized length scale ℓ for the size of the co-localized wave packets, we find that the total variational energy of the Bose-Fermi system is of the form

$$E \sim \ell^2 + \frac{1}{\ell^2} \pm \frac{1}{\ell^3} \pm \frac{1}{\ell^5}. \quad (1)$$

*nick.parker@ncl.ac.uk

The consecutive terms represent, respectively, radial potential energy, zero-point kinetic energy, s -wave interaction energy, and p -wave interaction energy. In the absence of p -wave interactions and for net attractive (negative) s -wave interactions, bright solitons are known to form but only as metastable states (local energy minima) prone to a collapse instability. We will show that the addition of repulsive (positive) p -wave interactions has a dramatic stabilizing effect on the soliton solutions, removing this collapse instability and promoting the solitons to ground states of the system (global energy minima).

In Sec. II we describe our methodology and derive the variational energy for the system up to and including the relevant p -wave interactions. In Sec. III A we consider the properties of the soliton solutions in the absence of p -wave interactions and show that our results are consistent with previous findings. In Sec. III B we progress to the main thrust of our work (to map out the properties in the presence of p -wave interactions) and demonstrate the capacity of p -wave interactions to stabilize against a collapse of the system. Note that we focus our results on a ^{87}Rb - ^{40}K mixture, due to the naturally large and attractive s -wave scattering length between the species [14,23,32], and fermion-fermion p -wave interactions, due to their capacity to be engineered experimentally [31]. Finally, in Sec. IV, we discuss and conclude our findings.

II. VARIATIONAL MODEL OF BOSE-FERMI SOLITONS

A. System overview and the variational ansatz

We consider a degenerate gas of identical fermions coexisting with a Bose-Einstein condensate of bosons, all at zero temperature. Neglecting quantum and thermal fluctuations, we will model the fermion and boson gases within the mean-field picture. Each gas is confined by an axially homogeneous waveguide potential $V_{B\{F\}}(\mathbf{r}) = \frac{1}{2}m_{B\{F\}}\omega_{B\{F\}}^2 r^2$, where $\omega_{B\{F\}}$ is the radial trap frequency experienced by the bosons {fermions} and $m_{B\{F\}}$ is the boson {fermion} mass. Due to the low energy of the atomic collisions, the s -wave and p -wave interactions are modelled by contact interactions characterized by a single length scale, the scattering length. Within the Bose gas, the atoms interact predominantly via s -wave scattering with characteristic length a_B (p -wave interactions are negligible). Within the Fermi gas, s -wave interactions are suppressed via the Pauli exclusion principle and the leading atomic interaction is p wave with a scattering length a_F [25]. For overlapping clouds, the bosons and fermions additionally interact with each other, predominantly via the s -wave interaction, of length scale a_{BFs} , but we will also include the corresponding p -wave interaction, with effective scattering length a_{BFp} [25].

Bright solitons require an attractive interaction to enable self-trapping of the wave. Here we shall consider the case where this interaction arises from the s -wave boson-fermion coupling. A rudimentary requirement is, thus, that the boson and fermion gases are overlapping in space and this enables us to assume the same ansatz for the boson and fermion density distributions. We will assume that the radial profile of the fermion and boson gases is a Gaussian. This is an exact result in the quasi-1D limit (formally expressed as $\hbar\omega_B \gg \mu_B$ and

$\hbar\omega_F \gg \mu_F$, where μ_B and μ_F are the chemical potentials of the boson gas and fermion gas, respectively [33]) for which the radial profile coincides with the Gaussian ground harmonic oscillator state.

The most obvious choice for a suitable axial profile is, by analogy to 1D bright bosonic soliton result, a sech-profile [34]. However, with this choice we are unable to obtain analytic solutions for the variational energies. Karpiuk *et al.* [18] pursued this choice numerically. Instead, to obtain an analytic form for the variational energies, we employ a Gaussian axial profile. From studies of bright BEC solitons it has been shown, first, that sech and Gaussian axial profiles give very similar results, and, second, that both forms of ansatz give very good agreement with more precise theoretical treatments, e.g., numerical solutions of the Gross-Pitaevskii equation [10,11]. We will, thus, consider the boson {fermion} density $n_{B\{F\}}$ to have a cylindrically symmetric Gaussian profile,

$$n_{B\{F\}}(\mathbf{r}) = \frac{N_{B\{F\}}}{\pi^{3/2}L_zL_r^2} \exp\left(-\frac{z^2}{L_z^2}\right) \exp\left(-\frac{r^2}{L_r^2}\right), \quad (2)$$

where L_r and L_z are the radial and axial sizes, respectively, and $N_{B\{F\}}$ is the number of bosons {fermions}. We consider that L_r and L_z are common for both the bosons and the fermions.

Note that the validity of the mean-field Gross-Pitaevskii model for the boson gas requires that $N_B \gg 1$. Furthermore, our description of the Fermi gas component is based on the Thomas-Fermi approximation which is valid for $N_F^{1/3} \gg 1$ [34]. We will only consider parameters that satisfy this large N limit.

B. Energetics of the system

We will consider the total energy density of the Bose-Fermi state $\varepsilon[n_B, n_F]$ to be the sum of the boson contribution $\varepsilon_B[n_B]$, fermion contribution $\varepsilon_F[n_F]$, and boson-fermion term $\varepsilon_{BF}[n_B, n_F]$ [25]. We will proceed by modeling each energy contribution of the Gaussian wave packets in turn. Note that the energy is the volume integral of the corresponding energy density $E = \int \varepsilon[n]dV$. For a different choice of ansatz and in the absence of p -wave interactions, Karpiuk *et al.* [18] followed a similar variational approach to explore Bose-Fermi soliton solutions.

1. Bosonic energy contribution

The energy density of the zero-temperature boson gas, interacting via s -wave interactions of scattering length a_B , is provided by the Gross-Pitaevskii model [34],

$$\varepsilon_B[n_B] = \frac{\hbar^2}{2m} |\nabla \sqrt{n_B}|^2 + V_B(\mathbf{r})n_B + \frac{2\pi\hbar^2 a_B}{m_B} n_B^2. \quad (3)$$

The terms of the right-hand side represent, respectively, the kinetic, potential, and interaction energies of the boson gas. For convenience we will express length in terms of the boson harmonic oscillator length $l_{\text{ho}} = \sqrt{\hbar/m_B\omega_B}$ and adopt dimensionless variational length scales $l_z = L_z/l_{\text{ho}}$ and $l_r = L_r/l_{\text{ho}}$. Furthermore, we rescale energy by the bosonic harmonic oscillator energy $\hbar\omega_B$ via $E \rightarrow E/(\hbar\omega_B)$. Substituting $n_B(\mathbf{r})$

into Eq. (3) and integrating over space, one arrives at the well-established expression for the total boson energy [34],

$$\frac{E_B}{N_B} = \frac{1}{2} \left(\frac{1}{l_r^2} + \frac{1}{2l_z^2} \right) + \frac{1}{2} l_r^2 + \frac{1}{\sqrt{2\pi}} \frac{a_B}{l_{ho}} \frac{N_B}{l_z l_r^2}. \quad (4)$$

We will find that the energetics of the full Bose-Fermi system [summarized in Eq. (1)] follow a similar pattern to this result and so it is pertinent to make some general observations. For $a_B > 0$ there is no well-defined energy minimum within this “energy landscape,” i.e., no static solution. However, the energy does become minimized in the unphysical limit $l_z \rightarrow \infty$, which represents the tendency of a wave packet therein to disperse. We will henceforth refer to this as the *dispersive instability*. For $a_B < 0$ the negative interaction term dominates over all other (positive) energy contributions in the limit $(l_r, l_z) \rightarrow (0, 0)$, i.e., the global energy minimum is a collapsed state of zero width. It is possible, for relatively weak attractive interactions, to support local energy minima in this system and, thus, static soliton solutions. However, for stronger attractive interactions, no local energy minima exist and the energy landscape decays monotonically as $(l_r, l_z) \rightarrow 0$. A wave packet in this system will tend toward this zero-width state. We will henceforth refer to this scenario as the *collapse instability*.

2. Fermionic energy contribution

Determination of the mean-field fermionic energy density in general requires solving N_F coupled Hartree-Fock equations. In this manner, Karpiuk *et al.* [17] successfully modelled BF soliton solutions, but the approach is only tractable for of the order of 10 fermions. Instead, we will adopt an analytic form for the fermion energy density derived by Roth and Feldmeier [25]. Employing the Thomas-Fermi approximation, this approach follows from deriving the energy density of a homogeneous fermionic system and replacing the fixed density with $n_F(\mathbf{r})$ (thus neglecting the contribution to the energy from density gradients). The Thomas-Fermi approximation is valid for the equilibrium state of a Fermi gas when the fermion wavelength is much smaller than the system size. For a trapped Fermi gas, it can be shown that this is satisfied when $N_F^{1/3} \gg 1$ [34]. In agreement with this, the Thomas-Fermi approximation has been shown to give an excellent mean-field description of BF mixtures (in close agreement with Hartree-Fock calculations) for $N_F \sim 1000$ [25,35]. Via this approach, the energy density of the fermions (potential, kinetic, and *p*-wave interaction terms, respectively) is [25],

$$\varepsilon_F[n_F] = V_F(\mathbf{r})n_F + \frac{3\hbar^2(6\pi^2)^{2/3}}{10m_F} n_F^{5/3} + \frac{(6\pi^2)^{5/3}}{5\pi m_F} \hbar^2 a_F^3 n_F^{8/3}, \quad (5)$$

where a_F is the *p*-wave contact interaction between fermions [25]. Inserting the Gaussian profile $n_F(\mathbf{r})$ and integrating gives the total fermionic energy,

$$\begin{aligned} \frac{E_F}{N_F} = & \alpha \frac{m_B}{m_F} \left(\frac{N_F}{l_z l_r^2} \right)^{2/3} + \frac{1}{2} \frac{m_F}{m_B} \left(\frac{\omega_F}{\omega_B} \right)^2 l_r^2 \\ & + 4\beta \frac{m_B}{m_F} \left(\frac{a_F}{l_{ho}} \right)^3 \left(\frac{N_F}{l_z l_r^2} \right)^{5/3}, \end{aligned} \quad (6)$$

where $\alpha = (9/50)6^{2/3}(3/5)^{1/2}\pi^{1/3} \approx 0.6743$ and $\beta = (3/160\pi^4)(3\pi/8)^{1/2}(6\pi^2)^{5/3} \approx 0.1880$.

3. Bose-Fermi energy contribution

Again, under the Thomas-Fermi approximation, the interaction energy density between the bosons and fermions $\varepsilon_{BF}[n_B, n_F]$ is [25],

$$\varepsilon_{BF}[n_B, n_F] = \frac{2\pi\hbar^2 a_{BFs}}{\mu} n_B n_F + \frac{(6\pi^2)^{5/3}}{20\pi\mu} \hbar^2 a_{BFp}^3 n_B n_F^{5/3}, \quad (7)$$

where a_{BFs} is the *s*-wave boson-fermion scattering coefficient, a_{BFp} is the *p*-wave scattering length, and $\mu = m_B m_F / (m_B + m_F)$. For the density profiles [Eq. (2)] the boson-fermion interaction energy is

$$\frac{E_{BF}}{N_B} = \frac{1}{\sqrt{2\pi}} \frac{a_{BFs}}{l_{ho}} \frac{m_B}{\mu} \frac{N_F}{l_z l_r^2} + \beta \frac{m_B}{\mu} \left(\frac{a_{BFp}}{l_{ho}} \right)^3 \left(\frac{N_F}{l_z l_r^2} \right)^{5/3}. \quad (8)$$

C. Energy landscapes and obtaining the variational solutions

The total energy of our Gaussian Bose-Fermi wave packets is given by $E = E_B + E_F + E_{BF}$. On fixing the experimental parameters (atom masses, atom numbers, scattering lengths, and trap frequencies), the energy becomes confined to being a function of only the wave-packet size parameters l_r and l_z . This function $E(l_r, l_z)$ can be visualized as an energy landscape in which the presence of an energy minimum represents a variational solution. In practice, we numerically define this energy landscape and perform a simple computational search for such energy minima. Note that an unphysical solution can occur at the origin representing the effect of collapse. It is unphysical in the sense that a real Bose-Fermi system cannot shrink to zero size; in reality, a collapse will eventually become halted by the surge of three-body losses as the gas densities rise. At most, only one physical solution is ever present in these energy landscapes. We denote the coordinates of such a variational solution by the coordinates l_z^0 and l_r^0 .

Where we map out regions of soliton solutions within a particular parameter space, e.g., $a_{BFs} - N_F$ space, this is done by randomly sampling combinations of these parameters. We typically restrict our numerical search to landscapes of extent $[0, 2]l_r \times [0, 10]l_z$.

D. Analytical limit: No *p*-wave interactions and $N_B \gg N_F$

We can gain a simplified analytic form for the total variational energy if we neglect *p*-wave interactions ($a_F = a_{BFp} = 0$) and assume $N_B \gg N_F$. The latter condition renders the fermion-fermion energy terms negligible and makes significant only terms involving N_B . The total variational energy then reduces to

$$\begin{aligned} \frac{E}{N_B} = & \frac{1}{2l_r^2} + \frac{1}{4l_z^2} \\ & + \frac{l_r^2}{2} + \left(N_B \frac{a_B}{l_{ho}} + \frac{a_{BFs}}{l_{ho}} \frac{m_B}{\mu} N_F \right) \frac{1}{\sqrt{2\pi} l_z l_r^2}. \end{aligned} \quad (9)$$

This form will enable us to gain physical intuition of the system and provide simple criteria for the existence of stable Bose-Fermi solitons. Importantly, it has the same form as the Gaussian variational energy of a purely bosonic gas [10] but with an effective s -wave scattering length given by [26]

$$a_{\text{eff}} = a_B + a_{BFs} \frac{N_F}{N_B} \left(\frac{m_F + m_B}{m_F} \right). \quad (10)$$

A rudimentary requirement for the ability to self-trap is that the net interactions are attractive ($a_{\text{eff}} < 0$). This places a lower bound on the ratio N_F/N_B for which Bose-Fermi solitons can be self-supported,

$$\frac{N_F}{N_B} > -\frac{a_B}{a_{BFs}} \left(\frac{m_F}{m_F + m_B} \right). \quad (11)$$

Furthermore, bright bosonic solitons are established to collapse when the scattering length is less than the critical value $a_B^c = k_c l_{\text{ho}}/N_B$. For a 3D Gaussian wave packet the dimensionless coefficient has been shown to be $k_c = -0.778$ [10] (for other shapes of wave packet the value differs but remains of the order of unity). This leads to an upper bound for the ratio N_F/N_B in order to prevent collapse of the system,

$$\frac{N_F}{N_B} < \frac{k_c l_{\text{ho}}}{N_B a_{BFs}} \left(\frac{m_F}{m_F + m_B} \right) - \frac{a_B}{a_{BFs}} \left(\frac{m_F}{m_F + m_B} \right). \quad (12)$$

From Eqs. (11) and (12) it is evident that the soliton solutions exist within a ‘‘window’’ of fermion atom number N_F whose width is,

$$\Delta N_F = \frac{k_c l_{\text{ho}}}{a_{BFs}} \left(\frac{m_F}{m_F + m_B} \right). \quad (13)$$

Equations (11)–(13) provide us with an estimate for the locality and range over which BF solitons solutions may exist. Equation (13) indicates that the width of the soliton bands can be extended by employing weaker radial trapping and weaker Bose-Fermi scattering length. However, we will find that the soliton bands are even more restricted if the condition $N_B/N_F \gg 1$ is removed. Indeed, the above equations predict the existence of soliton solutions at the native Bose-Fermi scattering length $a_{BFs} = -215a_0$. However, as we shall see, the full variational results predict that the soliton bands become vanishing narrow at this scattering length.

III. RESULTS

While our analytical results presented so far are applicable to any Bose-Fermi species, we will focus our ensuing results on a ^{87}Rb and ^{40}K mixture due to its naturally strong and attractive Bose-Fermi coupling and its prominent experimental occurrence to date [14,23]. We will assume that the atoms are spin-polarized and confined (in the radial direction) by a magnetic trap such that the trap frequencies are related via $\omega_F/\omega_B = (m_B/m_F)^{1/2}$. Throughout our results we fix the boson-boson s -wave scattering length to be the experimentally measured value of $a_B = 99a_0$ [36], where $a_0 = 5.3 \times 10^{-11}$ m is the Bohr radius. We will consider the radial trap frequency, boson and fermion atom numbers, and remaining scattering lengths to be variables. In the cases where we fix the boson-fermion s -wave scattering length, we take it to be its native value of $a_{BFs} = -215a_0$, as measured by Ferlaino

et al. [32]. Note that the strength of boson-boson interactions, boson-fermion interactions, and fermion-fermion interactions can be experimentally tuned, typically over many orders of magnitude, by using magnetic and optical fields to access interatomic scattering resonances. For example, magnetic Feshbach resonances have shown that for a ^{87}Rb - ^{40}K mixture a_{BF} can be precisely tuned over the range $[-1500a_0, 1500a_0]$ [37] while for ^{40}K the p -wave interaction cross section has been varied by over three orders of magnitude [31].

First, we will explore the soliton solutions in the absence of p -wave interactions. Following this, we will consider how p -wave interactions between fermions modify the soliton solutions. We will not explicitly present results for finite boson-fermion p -wave interactions but will comment on how they affect the system in Sec. IV.

A. Absence of p -wave interactions

1. Soliton bands in $N_F - a_{BFs}$ space

Figure 1(a) presents the soliton solutions in the parameter space of $a_{BFs} - N_F$ for 10^5 bosons and various radial trap frequencies [$\omega_B/2\pi = 10$ (green solid region), 100 (blue dotted region), and 1000 Hz (black dashed region)]. For each trap frequency, the soliton solutions exist in a narrow band in the $a_{BFs} < 0$ half-plane. (Note that on the scale of the figure these bands appear as lines.) Above each band, the system is unstable to dispersion and below the band it is unstable to collapse. Each band scales approximately as $-1/N_F$, as indicated by rearranging Eqs. (11) and (12). The bands are weakly dependent on trap frequency. Indeed, their differences are apparent only on a much more magnified scale [inset of Fig. 1(a)]. As ω_B is increased, the bands shift upward in a_{BFs} and become slightly narrower. The latter change is in qualitative agreement with Eqs. (11)–(13) which predict the band width to scale in proportion to $l_{\text{ho}} = \sqrt{\hbar/m\omega_B}$. Although not visible in Fig. 1(a), the bands become progressively narrower as N_F increases. Indeed, beyond some critical fermion number N_F^{crit} we cannot detect further solutions. This marks an important difference between the approximated analytic predictions of Eqs. (11)–(13) and the full variational solutions. For example, for trap frequencies $\omega_B/2\pi = 10, 100$, and 1000 and $N_F^{\text{crit}} \approx 760, 660$, and 620, respectively.

Within the soliton bands, the soliton radial size l_r^0 remains close to l_{ho} throughout. The axial size l_z^0 is infinite at its dispersive boundary and reduces as a_{BFs} is made more attractive, with the soliton becoming almost spherical at the point of collapse. This is qualitatively similar to the case for BEC bright solitons [10]. Figure 2 shows how the soliton bands change for different number of bosons [in both linear (a) and logarithmic plots (b)]. For increasing N_B the bands shift to more negative a_{BFs} and larger N_F , and the bands becomes wider as N_B is reduced.

Our numerical results predict that, for the numbers of bosons and fermions permitted by our model ($\gg 1$), soliton solutions do not occur at the native Bose-Fermi scattering length $a_{BFs} = -215a_0$. The soliton solutions exist only for scattering lengths $a_{BFs} \ll -215a_0$. However, our results show that as N_B and, by association, N_F [since the ratio N_B/N_F must remain within narrow bounds for soliton-supporting conditions to be met; see, e.g., Eqs. (11)–(13)] is decreased the soliton

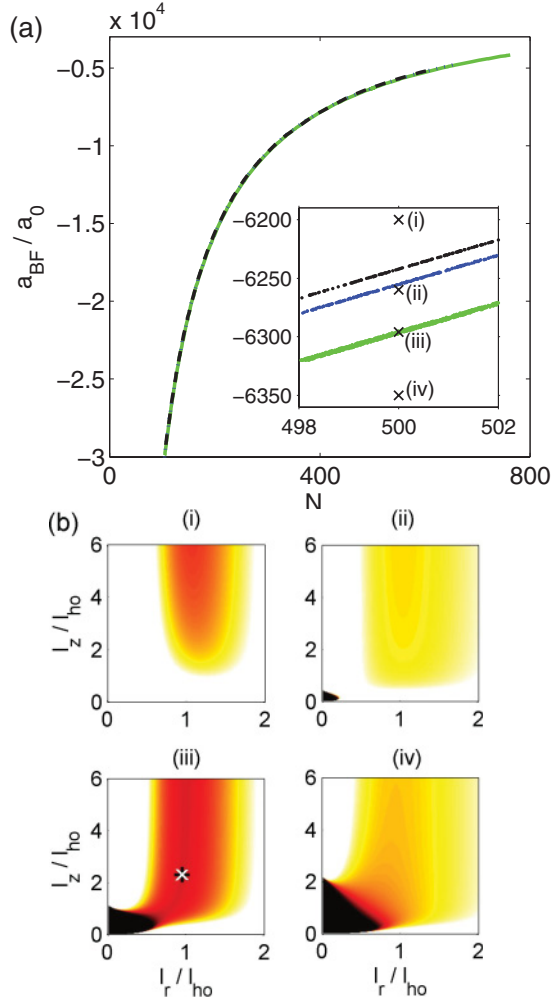


FIG. 1. (Color online) (a) The bands of soliton solutions in $a_{BFs} - N_F$ space for a ^{87}Rb - ^{40}K mixture with zero p -wave interaction. We present a fixed number of bosons $N_B = 10^5$ and various trap frequencies $\omega_B/2\pi = 10$ (green solid line), 100 (blue dotted line), and 1000 (black dashed line) Hz. The inset provides a close up of the soliton bands. (b) Energy landscapes ($\omega_B/2\pi = 10$ Hz, $N_F = 500$, and $N_B = 10^5$) showing four distinct regimes: (i) well above the soliton band ($a_{BFs} = -6200 a_0$), (ii) just above the band ($a_{BFs} = -6260 a_0$), (iii) within the band ($a_{BFs} = -6296 a_0$), and (iv) below the band ($a_{BFs} = -6350 a_0$). These plots corresponds to the crosses in (a). In (iii) the soliton solution is highlighted by the white cross.

solutions extend to smaller $|a_{BFs}|$. Indeed, if one were to extrapolate our predictions (beyond its strict regime of validity) to lower atom number, one could imagine that the soliton bands would reach $a_{BFs} = -215a_0$. Indeed, using a model valid for low atom numbers, Karpiuk *et al.* [17,18] predict the existence of BF solitons at the native $a_{BFs} = -215a_0$ for very low atom numbers.

2. Energy landscape regimes

To gain physical insight into the system, in Figs. 1(i)–1(iv) we present energy landscapes of four distinct regimes in this parameter space. While we present the landscapes for a specific set of parameters ($\omega_B/2\pi = 10$ Hz, $N_F = 500$, and $N_B =$

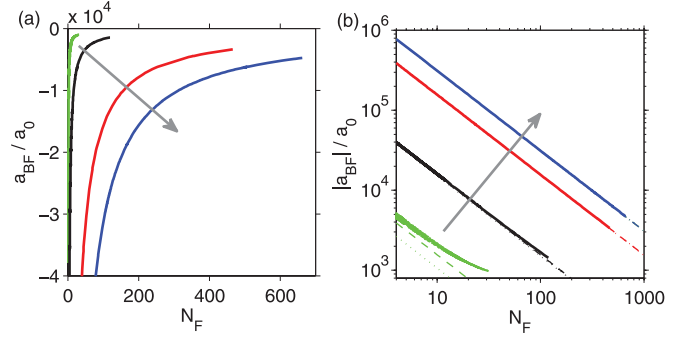


FIG. 2. (Color online) (a) The bands of soliton solutions in $a_{BFs} - N_F$ space for no p -wave contributions. We consider fixed trapping $\omega_B/2\pi = 100$ Hz and various boson numbers of $N_B = 500$ (green), 5000 (black), 50 000 (red), and 100 000 (blue). (b) Log-log plot of the soliton bands in (a), with the analytic predictions of Eqs. (11) (dashed line) and (12) (dotted line). The gray arrows indicate the direction of increasing N_B .

10^5), the qualitative behavior is generic. The location of each case is indicated in the inset of Fig. 1(a) by crosses. These four regimes [Figs. 1(i)–1(iv)] are as follows:

(i) Sufficiently above the soliton band, the net contact interactions are repulsive (positive) and the energy landscape consists of a downward “chute” aligned along the l_z axis. Any wave packet subjected to this system will disperse axially.

(ii) Just above the soliton band the net interactions become attractive (negative) and compete with the positive energy terms. The chute remains but the global energy minimum is now at the origin, where the energy diverges to $-\infty$. The attraction is insufficiently strong to support a soliton.

(iii) Within the band, the play-off between the interspecies attraction and repulsive zero-point kinetic energy leads to a local energy minimum at $[l_r^0, l_z^0]$ (highlighted by the black/white star), corresponding to the self-trapped soliton solution.

(iv) Below the soliton band the attractive interactions dominate the kinetic energy such that the only energy minimum is the global minimum at the origin, representing the collapse instability of the system.

3. Comparison to the simplified limit of Eqs. (11) and (12)

In Fig. 2(b) we present a comparison between the variational predictions for the soliton bands and the simplified analytic estimates provided by Eqs. (11) (dashed line) and (12) (dotted line). For ease of observing the differences between the two methods, the data are presented on a log-log plot. For a low number of bosons ($N_B = 500$) the variational solutions deviate from the predictions. However, for larger boson numbers the agreement is excellent. This is to be expected since these predictions assume $N_B/N_F \gg 1$. Indeed for $N_B = 5000$ and above, the simplified forms give very good predictions for the regimes of soliton solutions (indistinguishable from the full variational results on the scale of this figure).

An important difference, however, is that according to the analytical result, the width of the soliton band decreases as $1/N_F$, becoming vanishingly small only as $N_F \rightarrow \infty$. In contrast, the full variational solutions disappear beyond a finite N_F . Furthermore, numerically, the bands increase in width as

N_B is increased, whereas the analytical prediction for the band width is independent of N_B .

4. Comparison to findings elsewhere

We compare our findings thus far to the relevant results elsewhere. The works of Refs. [17,19] predict the existence of Bose-Fermi solitons when the Bose-Fermi interaction is sufficiently attractive, which is in qualitative agreement with our findings. However, the 1D setting of these studies prevented the modeling of collapse effects. To our knowledge the only work to have explored Bose-Fermi solitons in 3D is that of Karpiuk *et al.* [18]. Using mean-field Hartree-Fock simulations and variational modeling they showed that Bose-Fermi solitons exist over a range of atom numbers and Bose-Fermi interaction strengths, in agreement with our findings. In particular, they numerically explored a sech-Gaussian ansatz for the BF solitons and presented a phase diagram (Fig. 7 of Ref. [18]). We have verified that our methodology agrees to within 10% of their variational results. Such deviation is anticipated due, in this work, to the use of a Gaussian ansatz, which we note again allows an analytical prediction for the governing variational equation.

One cannot directly compare our results to the works on the stability of *trapped* Bose-Fermi mixtures due to the significant role of trapping. However, in Ref. [26] an expression is derived for the effective energy of the bosons in a (trapped) Bose-Fermi mixture up to *s*-wave scattering (Eq. (11) in Ref. [26]). As would be expected, for zero axial trapping, this is identical to our Eq. (9).

The previous studies of Bose-Fermi solitons have considered only *s*-wave interactions. The significant step in the new work presented here is the inclusion of *p*-wave interactions. As we show in the following, *p*-wave interactions can be used to modify the energy landscapes significantly such that soliton solutions become global energy minima of the system and the collapse instability is removed.

B. The role of *p*-wave fermion interactions

1. Soliton bands in $a_F - N_F$ space

We now consider the presence of fermion-fermion (*p*-wave) interactions. We fix the boson-fermion *s*-wave interaction to its natural value $a_{BFs} = -215a_0$ and explore the parameter space of $a_F - N_F$. The results are shown in Fig. 3 for fixed boson number $N_B = 10^5$ and various trap frequencies [$\omega_B/2\pi = 10$ (horizontal hatch), 100 (vertical hatch), and 1000 Hz (gray region)]. Recall that in the absence of *p*-wave interactions, no solitons were obtained for $a_{BFs} = -215a_0$. In contrast, in the presence of repulsive *p*-wave fermion-fermion interactions, we now see extensive regions of soliton solutions. The regions become larger for increased trap frequency. This change in size occurs due to a shift in the lower boundary of the regions; the upper boundary is insensitive to ω_B , as can be seen in Fig. 3(a).

This enhanced stability when *p*-wave fermion-fermion interactions are included arises from the fact that the fermion-fermion interaction term in Eq. (6) scales as ℓ^{-5} . Thus, if $a_F > 0$, this term ensures that the energy diverges to positive values as $\ell \rightarrow 0$ and completely removes the presence of a

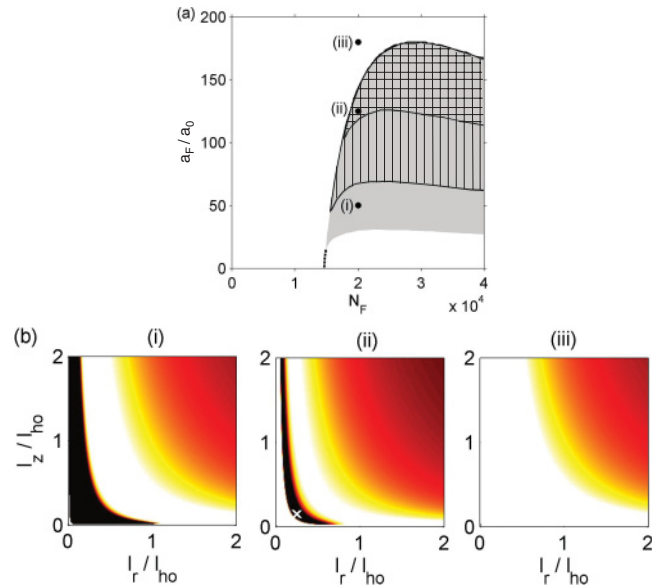


FIG. 3. (Color online) (a) Soliton bands in $a_F - N_F$ space for boson-fermion interaction $a_{BFs} = -215 a_0$ in the presence of fermion-fermion *p*-wave interactions. The number of bosons is fixed to $N_B = 100\,000$ and we present trap frequencies of $\omega_B/2\pi = 10$ (horizontal hatch), 100 (vertical hatch), and 1000 Hz (gray region). (b) Energy landscapes (for $\omega_B/2\pi = 100$ and $N_F = 20\,000$) of (i) below the band ($a_F = 50 a_0$), (ii) within the band ($a_F = 125 a_0$), and (iii) above the band ($a_F = 180 a_0$). The locations of these cases are indicated in plot (a).

collapse instability. This energetic behavior is demonstrated by the landscapes shown in Fig. 3(b).

(i) Below the relevant soliton band [e.g., the band shaded with vertical hatch in Fig. 3(a)] there is a large low-energy region in the landscape. However, the energy does diverge to $+\infty$ close to the origin [barely visible in Fig. 3(i)]. Note that there is no energy minimum in this landscape—the transition between the low-energy region and the divergent region is in the form of a saddle point.

(ii) Solutions become supported when the fermion-fermion interaction becomes larger and the play-off between all of the energy contributions generates a global minimum in the energy landscape (white cross).

(iii) Above the soliton band, the repulsive fermion-fermion interaction becomes so large that it makes the system fully dispersive.

Case (ii) is an intriguing prediction. It suggests that the presence of repulsive *p*-wave fermion interactions leads to solitons which are the *global* energy minimum of the system. This indicates that such solitons would be far more robust and stable than their bosonic counterparts, which are well known to exist as metastable states prone to an irremovable collapse instability.

In Fig. 4 we show how the bands change with the number of bosons. As the number of bosons decreases, the bands shift to lower N_F and become narrower. Indeed, the bands scale approximately as $1/N_B$, i.e., if we plot N_F/N_B on the x axis, the bands approximately overlap with each other.

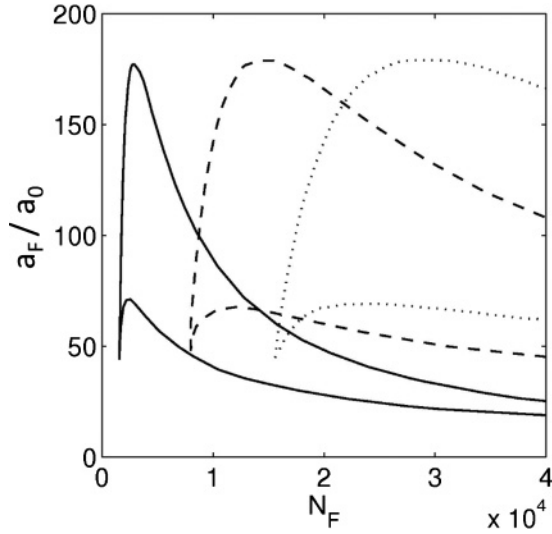


FIG. 4. Soliton bands in $a_F - N_F$ space for fixed trap frequency $\omega_B/2\pi = 100$ Hz and boson numbers of $N_B = 10\,000$ (solid), $50\,000$ (dashed), and $100\,000$ (dotted).

C. Soliton bands in $a_F - a_{BFs}$ space

The simultaneous manipulation of more than one scattering length has not been experimentally demonstrated. However, in principle, this could be possible through a combination of magnetic, optical, and confinement resonances. With this in mind and by way of exploring the soliton solutions further, we now turn to examine the regions of soliton solutions in $a_F - a_{BFs}$ space [Fig. 5(a)] for fixed N_B and N_F . We will see that the parameter space is particularly interesting because it offers the possibility of forming bright soliton solutions which are deep *global* minima. In this case, we observe complex-shaped regions of soliton solutions. This includes a large cusp shaped region in the $a_F > 0$ half-plane. Although not shown, this region extends to indefinitely negative a_{BFs} . Furthermore, the soliton region features narrow “fingers” which extend far into the $a_F < 0$ half-plane.

We discriminate six distinct regions in this parameter space which we interpret by reference to their typical energy landscapes presented in Fig. 5(b):

(i) Above this narrow band the landscape is dominated by dispersion with a localized collapse region, but no local minimum exists.

(ii) Within the soliton band there exists a shallow energy minimum [case (ii)] adjacent to the collapse and dispersive regions.

(iii) Below the soliton band the whole landscape is unstable to collapse.

(iv) and (v) In the regions containing points (iv) and (v) there is no collapse region at the origin and there exists a well-localized and deep energy minimum denoting a soliton solution.

(vi) This region is dispersive due to the dominance of repulsive interactions.

Regions (i)–(iii), and (vi) possess energy landscapes which are analogous to those seen in Fig. 1(b). However, the most intriguing regions are (iv) and (v). These solutions are the most common type that exist in this parameter space. Like the

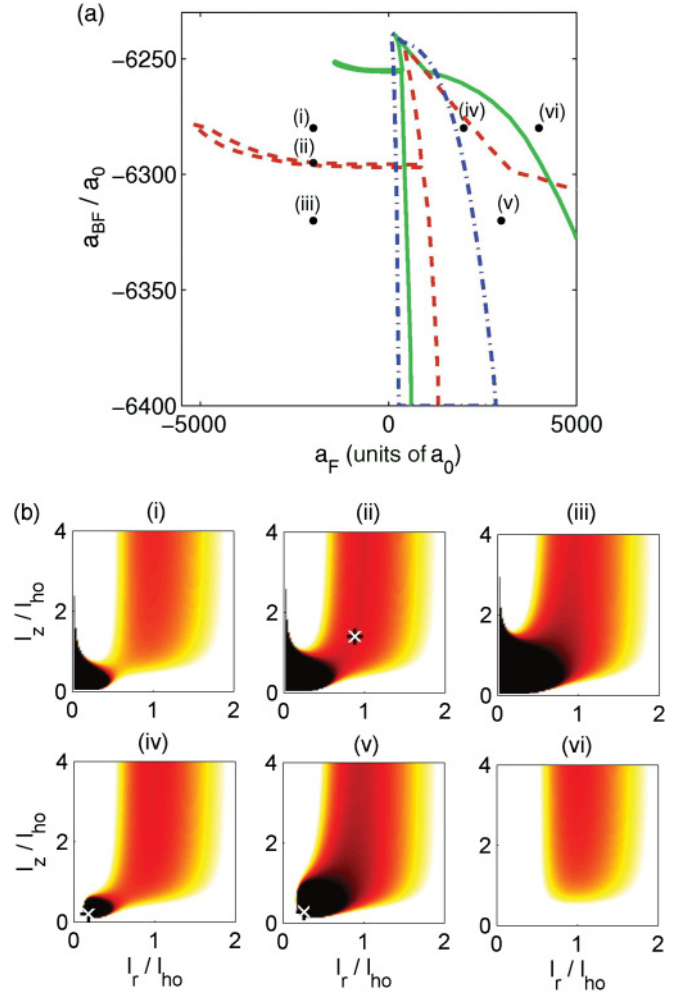


FIG. 5. (Color online) Soliton bands (as shown by their boundary lines) in the parameter space of a_F and a_{BFs} . (a) We fix $N_B = 100\,000$ and $N_F = 500$, and use $\omega_B/2\pi = 10$ (red dashed line), 100 (green solid line), and 1000 (blue dot-dashed line) Hz. (b) Energy landscapes for the $\omega_B/2\pi = 10$ case at the points (i) $a_F = -2000 a_0$, $a_{BFs} = -6280 a_0$; (ii) $a_F = -2000 a_0$, $a_{BFs} = -6295 a_0$; (iii) $a_F = -2000 a_0$, $a_{BFs} = -6320 a_0$; (iv) $a_F = 2000 a_0$, $a_{BFs} = -6280 a_0$; (v) $a_F = 3000 a_0$, $a_{BFs} = -6320 a_0$; and (vi) $a_F = 4000 a_0$, $a_{BFs} = -6280 a_0$. These points are denoted in (a).

observation in Fig. 3(ii), the soliton now becomes the *global* energy minimum of the system. However, these landscapes are strikingly well localized and deep. The depth of this minimum is typically of the order of $100 \hbar\omega_B$. For a comparison, for a bright bosonic soliton the depth of the energy minima is of the order of $0.1 \hbar\omega_B$. Within the context of our scaling solutions (fixed Gaussian shape), this depth and narrowness of the energy minima indicate extreme stability of the solutions to shape modification, including collapse and dispersion.

For completeness, Fig. 6 demonstrates how these extensive soliton regions in $a_F - a_{BFs}$ space become modified for different N_B . The presence of the “fingers” is sensitive to N_B but the main region of solutions persists, albeit shifting to more negative a_{BFs} with increasing N_B .

While here we have limited our study to the *p*-wave interactions of only the fermions, the same qualitative soliton regimes and solutions are obtained if the *p*-wave boson-fermion

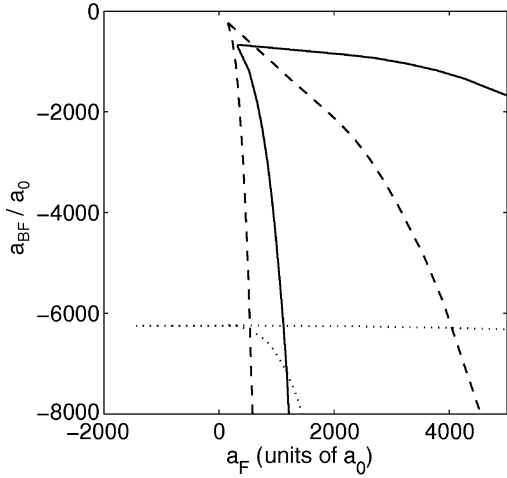


FIG. 6. Soliton bands in the parameter space $a_F - a_{BFs}$ (shown by their boundary lines). We fix $\omega_B/2\pi = 100$ Hz and $N_F = 500$ and consider $N_B = 1000$ (dashed line), 10 000 (solid line), and 100 000 (dotted line).

interaction is included instead (or, indeed, if both are included). This is because the p -wave fermion-boson interaction has the same functional form (scaling as ℓ^{-5}).

IV. DISCUSSION AND CONCLUSION

Our results show that in the absence of p -wave contributions the range of soliton solutions is rather limited, being confined to narrow bands in the $a_{BF} - N_F$ space. Indeed, the solutions behave similarly to bright bosonic solitons but with an effective scattering length. While reducing the radial confinement widens the soliton bands, this also makes the system more prone to collective excitations which may disrupt the soliton. For a ^{87}Rb - ^{40}K mixture and in the validity regime of our approach ($N_B, N_F \gg 1$) we cannot locate soliton solutions at the native boson-fermion scattering length of $-215 a_0$. Values of around $-1000 a_0$ are required to reach a soliton band at these atom numbers (indeed, the work of Karpiuk *et al.* demonstrated that atom numbers of order unity are required to support Bose-Fermi solitons at the native ^{87}Rb - ^{40}K scattering length). While the scattering length can be engineered to such large values through scattering resonance tuning [37], the ensuing soliton bands appear to be so narrow that experimentally locating them is likely to be problematic. Furthermore, there remains a collapse instability in the system and the ratio of bosons to fermions is constrained to small values. In contrast, the presence of repulsive p -wave fermion-fermion interactions has a dramatic stabilizing effect on the system. This can lead to a removal of the collapse instability such that the soliton solutions become *global* energy minima. We find extensive soliton regimes, in which the soliton minima

are extremely deep, suggesting that they may form soliton structures that are considerably more robust than in the absence of p -wave interactions. The p -wave interaction also provides a strong tuning parameter, enabling the boson-fermion ratio to be dramatically varied. Importantly, for a potential experimental realization of BF solitons, we find extensive soliton solutions at the native boson-fermion interaction and with only moderate fermionic interactions.

The remarkable capacity of repulsive p -wave interactions to remove the collapse instability stems from the scaling behavior of its energy contribution. Denoting a generalized length scale of the Gaussian wave packet as ℓ , the total variational energy of the Bose-Fermi system is of the form

$$E \sim \ell^2 + \frac{1}{\ell^2} \pm \frac{1}{\ell^3} \pm \frac{1}{\ell^5}. \quad (14)$$

The first two terms, the kinetic and potential energy terms, are always positive. The last two terms, the s -wave and p -wave interaction energies, respectively, may be positive or negative. In the absence of p -wave interactions, a negative s -wave term will cause the energy to diverge to $-\infty$ as $\ell \rightarrow 0$, signifying the presence of the collapse instability. For nonzero p -wave interactions, the p -wave term dictates the fate of the system as $\ell \rightarrow 0$ and, importantly, for positive p -wave interactions the collapse instability is completely removed.

It is important to note that this scaling behavior originates from the Thomas-Fermi approximation and so is not limited to Gaussian wave packets. Consider homogeneous Bose and Fermi gases in a large hard-wall box of volume ℓ^3 . It is trivial to see from Eqs. (3) and (5) that the energy scales as above, minus the ℓ^2 term. Thus it is clear that the capacity of repulsive p -wave interactions to stabilize against collapse will extend to trapped Bose-Fermi mixtures in general.

While we have presented results for p -wave interactions in only the fermion-fermion case, we find qualitatively similar soliton regions, landscapes, and conclusions when including boson-fermion p -wave interactions instead. This is because the same energy scaling discussed above applies.

In conclusion, according to a variational model valid for large atom number, the presence of repulsive p -wave interactions in Bose-Fermi mixtures removes the collapse instability and leads to stable, robust bright soliton stationary states that are global energy minima of the system. We have discussed specifically the boson-fermion pairing of ^{87}Rb and ^{40}K , but the stabilizing effect of repulsive p -wave interactions should apply across all ultracold Bose-Fermi mixtures. Given that the collapse instability has proved a major hindrance to the controlled generation, manipulation, and interaction of matter-wave solitons to date, these more stable p -wave entities may provide a more versatile route to explore and exploit the special characteristics of solitons.

- [1] J. S. Russell, in *Report on Waves, Report of the Fourteenth Meeting of the British Association for the Advancement of Science* (John Murray, London, 1844), pp. 311–390.
 [2] A. A. Levchenko *et al.*, *JETP Lett.* **65**, 573 (1997).

- [3] G. I. Stegeman and M. Segev, *Science* **286**, 1518 (1999).
 [4] L. Khaykovich *et al.*, *Science* **296**, 1290 (2002).
 [5] K. E. Strecker *et al.*, *Nature* **417**, 150 (2002).

- [6] S. L. Cornish, S. T. Thompson, and C. E. Wieman, *Phys. Rev. Lett.* **96**, 170401 (2006).
- [7] N. G. Parker, A. M. Martin, S. L. Cornish, and C. S. Adams, *J. Phys. B* **41**, 045303 (2008).
- [8] T. P. Billam, S. L. Cornish, and S. A. Gardiner, *Phys. Rev. A* **83**, 041602(R) (2011).
- [9] S. L. Cornish, N. G. Parker, A. M. Martin, T. Judd, M. Fromhold, and C. S. Adams, *Physica D* **238**, 1299 (2009).
- [10] V. M. Perez-Garcia, H. Michinel, and H. Herrero, *Phys. Rev. A* **57**, 3837 (1998); N. G. Parker, S. L. Cornish, C. S. Adams, and A. M. Martin, *J. Phys. B* **40**, 3127 (2007); N. G. Parker, A. M. Martin, C. S. Adams, and S. L. Cornish, *Physica D* **238**, 1456 (2009).
- [11] L. D. Carr and Y. Castin, *Phys. Rev. A* **66**, 063602 (2002).
- [12] A. G. Truscott *et al.*, *Science* **291**, 2570 (2001); F. Schreck, L. Khaykovich, K. L. Corwin, G. Ferrari, T. Bourdel, J. Cubizolles, and C. Salomon, *Phys. Rev. Lett.* **87**, 080403 (2001).
- [13] Z. Hadzibabic, C. A. Stan, K. Dieckmann, S. Gupta, M. W. Zwierlein, A. Gorlitz, and W. Ketterle, *Phys. Rev. Lett.* **88**, 160401 (2002).
- [14] G. Roati, F. Riboli, G. Modugno, and M. Inguscio, *Phys. Rev. Lett.* **89**, 150403 (2002); S. Inouye, J. Goldwin, M. L. Olsen, C. Ticknor, J. L. Bohn, and D. S. Jin, *ibid.* **93**, 183201 (2004); C. Ospelkaus, S. Ospelkaus, K. Sengstock, and K. Bongs, *ibid.* **96**, 020401 (2006); C. Klempt *et al.*, *Eur. Phys. J. D* **48**, 121 (2008).
- [15] T. Fukuhara, S. Sugawa, Y. Takasu, and Y. Takahashi, *Phys. Rev. A* **79**, 021601 (2009).
- [16] M. K. Tey, S. Stellmer, R. Grimm, and F. Schreck, *Phys. Rev. A* **82**, 011608 (2010).
- [17] T. Karpiuk, K. Brewczyk, S. Ospelkaus-Schwarzer, K. Bongs, M. Gajda, and K. Rzkazewski, *Phys. Rev. Lett.* **93**, 100401 (2004).
- [18] T. Karpiuk, M. Brewczyk, and K. Rzkazewski, *Phys. Rev. A* **73**, 053602 (2006).
- [19] S. K. Adhikari, *Phys. Rev. A* **72**, 053608 (2005); L. Salasnich, S. K. Adhikari, and F. Toigo, *ibid.* **75**, 023616 (2007); S. K. Adhikari and L. Salasnich, *ibid.* **76**, 023612 (2007).
- [20] M. Salerno, *Phys. Rev. A* **72**, 063602 (2005); S. K. Adhikari and B. A. Malomed, *ibid.* **76**, 043626 (2007); Yu. V. Bludov, J. Santhanam, V. M. Kenkre, and V. V. Konotop, *ibid.* **74**, 043620 (2006).
- [21] J. Santhanam, V. M. Kenkre, and V. V. Konotop, *Phys. Rev. A* **73**, 013612 (2006).
- [22] P. A. Ruprecht, M. J. Holland, K. Burnett, and M. Edwards, *Phys. Rev. A* **51**, 4704 (1995); J. L. Roberts, N. R. Claussen, S. L. Cornish, E. A. Donley, E. A. Cornell, and C. E. Wieman, *Phys. Rev. Lett.* **86**, 4211 (2001); A. Gammal, T. Frederico, and L. Tomio, *Phys. Rev. A* **64**, 055602 (2001).
- [23] G. Modugno, G. Roati, F. Riboli, F. Ferlaino, R. J. Brecha, and M. Inguscio, *Science* **297**, 2240 (2002).
- [24] K. Molmer, *Phys. Rev. Lett.* **80**, 1804 (1998); T. Miyakawa, T. Suzuki, and H. Yabu, *Phys. Rev. A* **64**, 033611 (2001); A. M. Belemuk, V. N. Ryzhov, and S. T. Chui, *ibid.* **76**, 013609 (2007); S. Röthel and A. Pelster, *Eur. Phys. J. B* **59**, 343 (2007).
- [25] R. Roth and H. Feldmeier, *Phys. Rev. A* **64**, 043603 (2001); **65**, 021603(R) (2002); R. Roth, *ibid.* **66**, 013614 (2002).
- [26] T. Karpiuk, M. Brewczyk, M. Gajda, and K. Rzakewski, *J. Phys. B* **38**, L215 (2005).
- [27] X. J. Liu, M. Modugno, and H. Hu, *Phys. Rev. A* **68**, 053605 (2003).
- [28] H. Saito and M. Ueda, *Phys. Rev. Lett.* **90**, 040403 (2003); F. K. Abdullaev, J. G. Caputo, R. A. Kraenkel, and B. A. Malomed, *Phys. Rev. A* **67**, 013605 (2003); S. K. Adhikari, *ibid.* **69**, 063613 (2004); G. D. Montesinos, V. M. Perez-Garcia, and P. J. Torres, *Physica D* **191**, 193 (2004); V. V. Konotop and P. Pacciani, *Phys. Rev. Lett.* **94**, 240405 (2005); A. Itin, T. Morishita, and S. Watanabe, *Phys. Rev. A* **74**, 033613 (2006); G. Filatrella, B. A. Malomed, and L. Salasnich, *ibid.* **79**, 045602 (2009).
- [29] F. Dalfovo and S. Stringari, *Phys. Rev. A* **53**, 2477 (1996); S. K. Adhikari, *Phys. Rev. E* **65**, 016703 (2001); *Phys. Rev. A* **66**, 043601 (2002); *New J. Phys.* **5**, 137 (2003); N. A. Jamaludin, N. G. Parker, and A. M. Martin, *Phys. Rev. A* **77**, 051603(R) (2008); **83**, 059910(E) (2011); M. C. Tsatsos, A. I. Streltsov, O. E. Alon, and L. S. Cederbaum, *ibid.* **82**, 033613 (2010); J. Abdullaev, A. S. Desyatnikov, and E. A. Ostrovskaya, *J. Opt.* **13**, 064023 (2011).
- [30] L. S. Cederbaum, A. I. Streltsov, and O. E. Alon, *Phys. Rev. Lett.* **100**, 040402 (2008).
- [31] C. A. Regal, C. Ticknor, J. L. Bohn, and D. S. Jin, *Phys. Rev. Lett.* **90**, 053201 (2003).
- [32] F. Ferlaino, C. Derrico, G. Roati, M. Zaccanti, M. Inguscio, G. Modugno, and A. Simoni, *Phys. Rev. A* **73**, 040702(R) (2006); **74**, 039903(E) (2006).
- [33] K. K. Das, *Phys. Rev. Lett.* **90**, 170403 (2003).
- [34] C. J. Pethick and H. Smith, *Bose-Einstein Condensation in Dilute Gases* (Cambridge University Press, Cambridge, 2001).
- [35] N. Nygaard and K. Molmer, *Phys. Rev. A* **59**, 2974 (1999).
- [36] E. G. M. van Kempen, S. J. J. M. F. Kokkelmans, D. J. Heinzen, and B. J. Verhaar, *Phys. Rev. Lett.* **88**, 093201 (2002).
- [37] C. Klempt, T. Henninger, O. Topic, J. Will, W. Ertmer, E. Tiemann, and J. Arlt, *Phys. Rev. A* **76**, 020701(R) (2007).